nternational Journal of Mining and Geological Engineering 1990, 8, 287–304

Yield pillars for stress control in longwall mines – case study SUNNYSIDE

K.Y. HARAMY and R.O. KNEISLEY

Mining engineer, Denver Research Center, Bureau of Mines, PO Box 20586, Denver, CO 80225, USA

Received 8 May 1990

Summary

The demand for increased productivity and the problems associated with mining at greater depths have increased the interest in using the yield pillar concept in the United States. This paper summarizes chain pillar behaviour in a mine that historically experienced coal bumps in both room-and-pillar and longwall sections. Results indicate that, generally, the chain pillars yield as designed, but that yielding occurred either after development or with approach of the longwall face. The Bureau of Mines investigated several yield pillar design approaches to possibly explain observed differences in pillar behaviour. These approaches suggest that very localized conditions, such as coal and rock properties, cover depth, and extraction height, may influence the behaviour of any one pillar. At this mine, yielding chain pillars result in de-stressing of the longwall entries and the transfer of potentially dangerous stress concentrations to adjacent panels. Pre-longwall-mining behaviour indicates the existence of a pressure arch, the width of which increases with depth. Results indicate that use of yield pillars improves stress control, reduces bump potential, and increases resource recovery.

Keywords: Yield pillars, longwall mining, coal mining, pillar design, rock mechanics.

Introduction

A yielding pillar is defined as a pillar that yields or fails upon isolation from the coal seam. The yield pillar allows a general lowering of the roof and subsequent transfer of the overburden load onto neighbouring mine structures. The yield pillar concept is not new, and in general, it has many advantages. Designing yield pillars rather than large pillars in longwall sections can result in improved ground control conditions and increased coal recovery. It also can have a positive effect on surface subsidence. Many researchers have proven that the design of longwall entries using yield pillars or the combination of yield pillars and large pillars is effective in protecting the entries from high stress concentrations.

Mining at great depths is associated with ground control problems caused by high stress concentrations. This has increased the interest in the yield pillar concept to redistribute stresses away from the entries. Researchers have developed theories for designing yield pillars in underground longwall mines. The objective of this study is to evaluate a yield pillar design using field measurements and to compare the field data with available theories.

0269–0136/90 $03.00+.12

Mine history

Coal mining in the Utah coalfields in Carbon and Emery Counties has a long association with the mountain bump problem. The Sunnyside mines, among the oldest and most extensively worked in the area, have a history coal of bumps (Lindsay, 1963). Natural conditions conducive to bumps include great depth, presently about 2500 ft; rapid variation of relief; tectonic movement associated with extensive faulting; and massive sandstone strata above and below the coalbeds (Jackson, 1971; Wong, 1985). One 200-ft (60 m)-thick sandstone layer, approximately 150 ft (45 m) above the coalbeds, creates widespread disturbances on active sections upon failure or when loaded (Jackson, 1971). Although the roof consists primarily of sandstone, major bumps are often accompanied by extensive roof falls of the very poor, immediate roof shale and by methane inflows.

At this mine, violent bumps occurred when the pillar line retreated under the upper bed pillar remnants. The sudden failure of the upper bed pillars resulted not only in lower bed bumps, but also in irregular weight distribution, punching through of pillar stumps, and erratic roof action (Sunnyside, 1962). Costs associated with remedial work often resulted in bypassing or abandoning problem areas, which only aggravated the bump problem (Peperakis, 1968). Longwall mining was introduced in 1961 to alleviate severe coal bumps that occurred during room-and-pillar mining (Lindsay, 1962; Ross, 1974). The initial longwall was set up in the No. 3 mine, originally opened in 1896, that worked both the 4 to 6 ft (1.2 to 1.8 m) upper and 6 to 10 ft (1.8 to 3 m) lower beds.

The initial longwall panel, 1000 ft (300 m) long by 300 ft (90 m) wide, used previously driven entries only 20 ft (6 m) below the upper bed pillars (Peperakis, 1968). The first panel experienced very heavy pressure and required arches, timbers, and additional bolts t(maintain the panel entries. Two major bumps, 5 min apart, occurred on the first panel. The first event damaged 1200 ft (360 m) of the haulage entry; the second bump, caused by a combination of upper bed pillar collapse and caving of a previously hanging roof, struck the entire face and derailed the shearer. The first three panels experienced ground control problems with three-entry systems; major roof support was required, especially when mining under upper bed pillars (Peperakis, 1968). Experience with the evolved two-entry system at this mine has been favourable. Entries have stood well and have not experienced high pressure. The two-entry systems have experienced less bumping, and the small, single chain pillars tend to crush out during longwall retreat (Peperakis, 1968; Jackson, 1971).

Geology

Physiographically, the area is part of the Colorado Plateau province. The Sunnyside mines are located at the base of the western Book Cliffs Field. The cliffs rise 1000 to 1500 ft (300 to 450 m) and are cut by numerous steep canyons (Scheibner, 1979). Cover at the mine ranges from 1500 to over 2000 ft 450 to 750 m). The main coal-producing unit, the Blackhawk Formation, is underlain by the Mancos Shale and overlain by the Castlegate Sandstone. The Blackhawk Formation, approximately 700 ft (210 m) thick, consists of three members as shown in Fig. 1. The Sunnyside Member, 100 to 150 ft (30 to 45 m) thick, immediately underlays the Sunnyside coalbed and consists of interbedded sandstone and siltstone at its base and a medium grain sandstone at the top (Scheibner, 1979). The upper unit is a 250 to

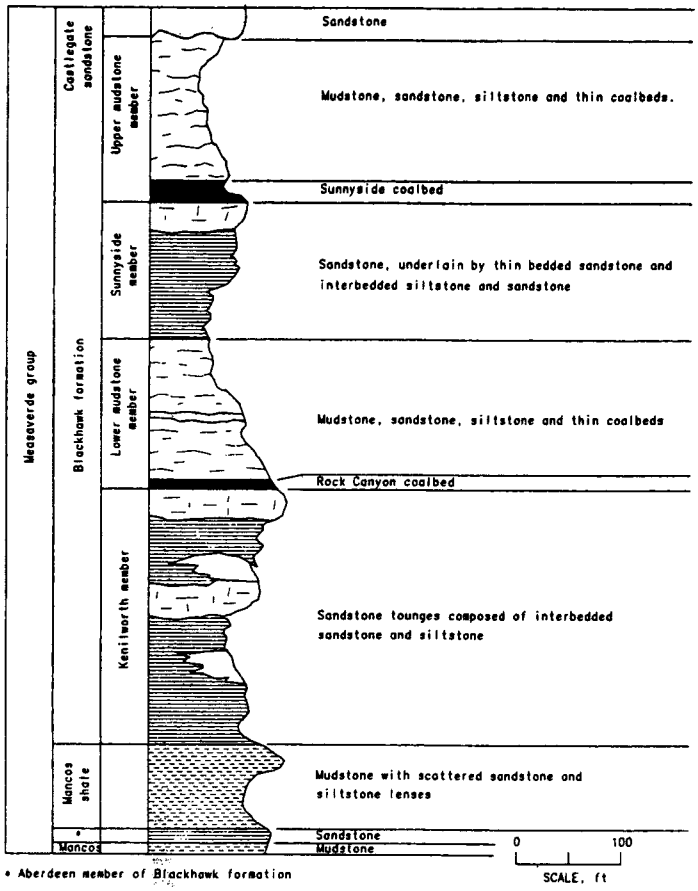

Fig. 1. Mine geological column (after Scheibner, 1979) (1 ft = 0.3048 m)

300 ft (75 to 90 m) thick member consisting of sandy siltstone, lenticular sandstones, mudstones, and the upper and lower Sunnyside coalbeds.

In the No. 1 mine, the upper and lower seams are considered splits of the Sunnyside coalbed. The split is not present everywhere, but in some areas ranges up to 75 ft (22 m). Above and below the upper and lower coalbeds are irregular, thin coalbeds, and intertongued with the seams are beds of sandstone and siltstone. The lower coalbed is very hard, relatively unfractured, and forms a competent rib; the upper bed, while also hard, often shatters vertically into long, thin fragments. When combined in a single seam, the beds generally maintain their characteristic appearance. (Scheibner, 1979).

Osterwald (1962) reports that bumping occurs in workings that diverge at large angles from the orientation of predominant fractures – faults, joints, and cleats within the coal. If one of the principal stress directions in a pillar intersects a fault, joint or fracture at a small angle, slippage will occur, but if intersecting at a large angle, a large stress and a violent bump may occur. Stress concentrations in a reactivated pre-mining fracture parellel to a rib will concentrate in the small volume of coal between the rib and fracture. Bumping, if any, will occur before large stress accumulates. If the fracture makes a large angle to the rib, more stress will be stored, and the failure will be more violent (Osterwald, 1962).

Rock mechanics investigation

Sunnyside No. 1 Mine was selected as a test site because of its history of bump occurrences. Since high stress is a problem common to bump-prone mines, the instrumentation programme was developed to monitor stress buildups in adjacent longwall panels, chain pillars, and on selected face supports (Haramy and McDonnell, 1988). This paper summarizes only those results from the panels and chain pillars.

Test site location and instrumentation

Instrumentation was installed in two test areas of the 20th Left longwall panel headgate entries: stations A and B near crosscut 42 and stations C and D near crosscut 13. Stations A and B were under approximately 1500 ft (450 m) of cover, and stations C and D were under approximately 2000 ft (600 m) of cover. These sites were selected to compare entry system behaviour under different depths. Figure 2 shows the general instrumentation locations with overburden contours. Overburden above the 20th left panel ranged between 1300 ft (390 m) and approximately 2000 ft (600 m). The panel lies perpendicular to several ridges, and overburden thickness changed frequently and rapidly as the panel retreated. The 20th Left panel was 550 ft (165 m) wide by 5500 ft (1650 m) long and utilized a two-entry system with yielding chain pillars. One goal of this study was to quantify the behaviour of these yielding chain pillars.

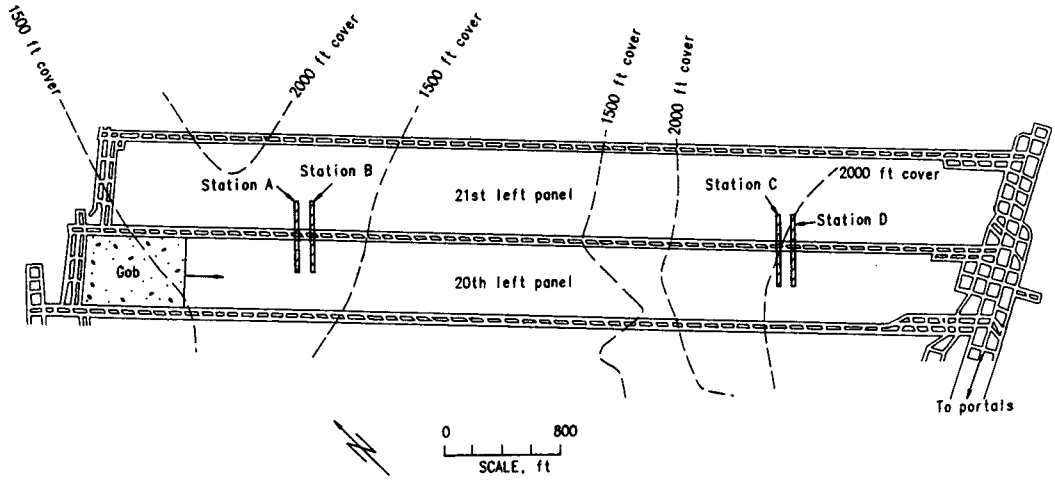

Fig. 2. Instrumentation locations. (1 ft = 0.3048 m)

Instrumentation site details are shown in Figs 3 and 4; pressure changes were measured using borehole pressure cells (BPC) and cylindrical pressure cells (CPC) installed at a seating pressure of 1500 p.s.i. or 2000 p.s.i. (10 or 20 MN/m^2), which is equivalent to the estimated overburden pressures at sites A and B, and C and D, respectively. The BPC flat

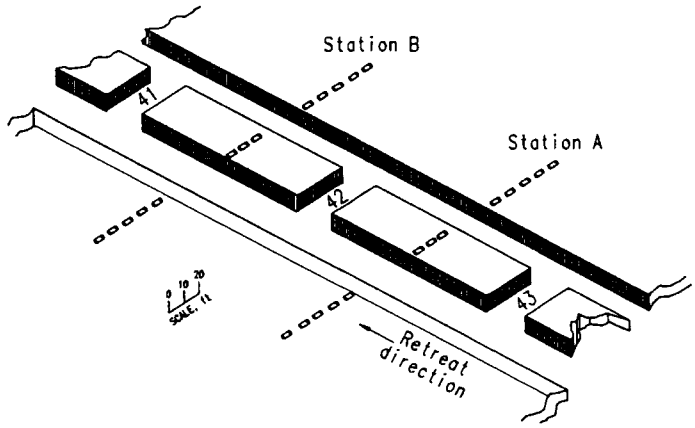

Fig. 3. Detailed instrumentation locations, sites A and B (1 ft = 0.3048 m)

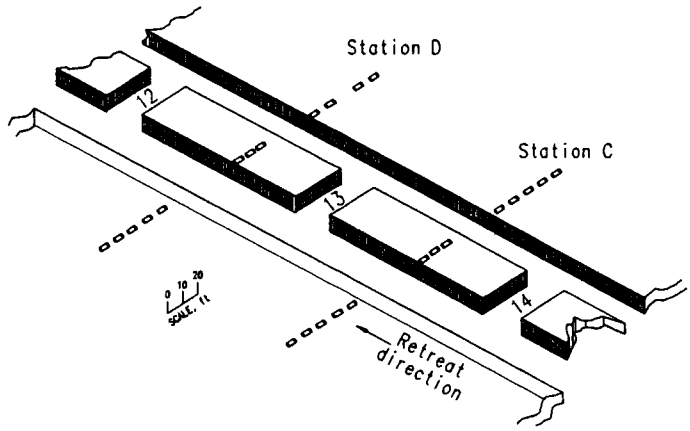

Fig. 4. Detailed instrumentation locations, sites C and D (1 ft = 0.3048 m)

hydraulic cell is encapsulated in a sand-cement mortar and is used to measure rock pressure changes normal to the plane of the cell. The CPC includes a steel rod enclosed by a copper jacket and is used to measure radial pressure changes in a borehole.

Site stratigraphy and physical properties test results

Boreholes were drilled into the headgate entry roof of crosscuts 12, 19, 21 and 23, and into the floor of crosscut 12 to determine changes in lithology and to obtain core for physical properties testing.

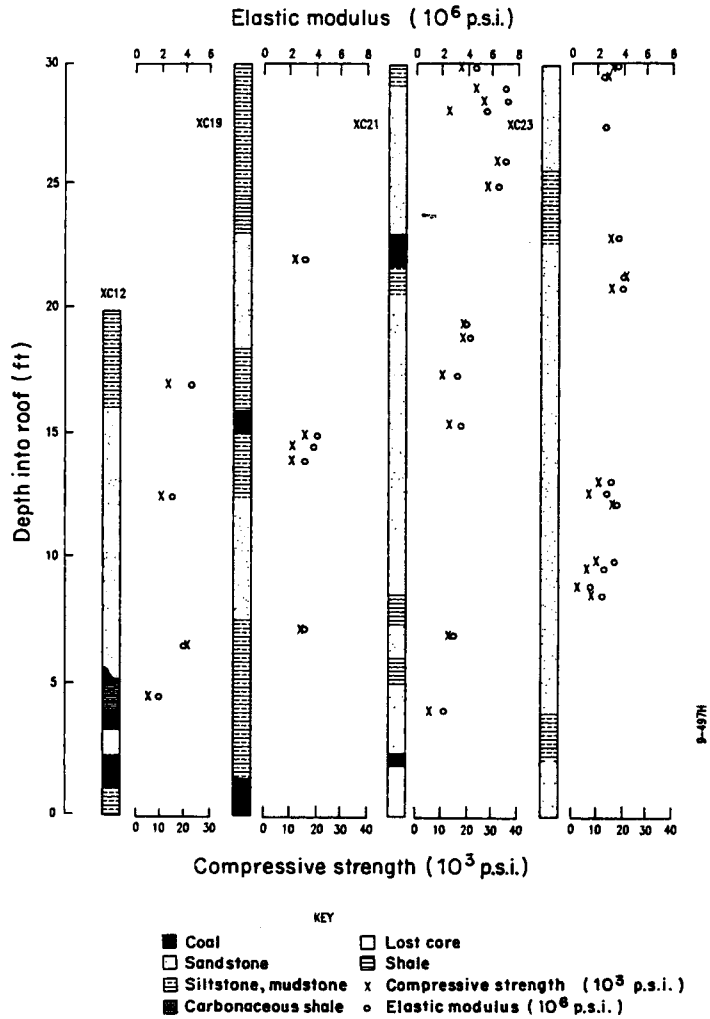

Fig. 5. Mine-roof stratigraphy and physical property data (1 ft = 0.3048 m; 1000 p.s.i. = 6.895 MN/m^2)

Figures 5 and 6 summarize roof and floor stratigraphy and uniaxial test results. Although the first 5 ft (1.5 m) of immediate roof indicates some variability between boreholes, the roof consists primarily of sandstone and siltstone. The immediate floor consists of thin coal, shale, siltstone, and carbonaceous shale resting on a massive sandstone that begins about 13 ft (3.9 m) below the coal seam.

Triaxial results are summarized in Fig. 7. Selected strata were tested to failure under confining pressures ranging from 0 p.s.i. to 2000 p.s.i. Linear regression analyses of the data was used to determine the intercept which is equivalent to the unconfined compressive strength. The slope of the best-fit line which is equivalent to the triaxial factor was determined. The triaxial and uniaxial test results, are used in the comparison of pillar behaviour to pillar design theories.

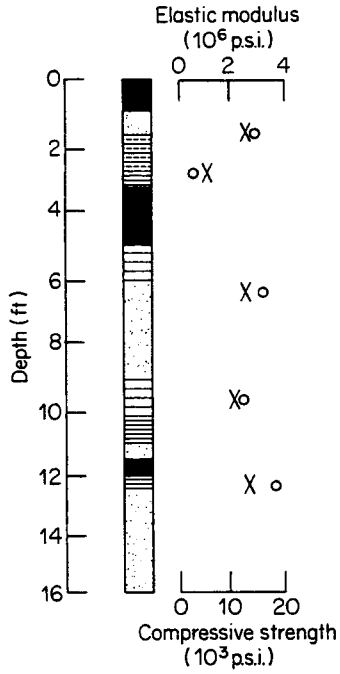

Fig. 6. Mine-floor stratigraphy and physical property data (1 ft = 0.3048 m; 1000 p.s.i. = 6.895 MN/m²)

Results

Borehole pressure cells (BPCs) were installed in the chain pillar and adjacent panels to measure vertical pressures and vertical pressure changes as mining approached. This summary includes analyses of forward abutment pressures, pillar–panel load transfer, and comparison of observed chain pillar behaviour to several yield pillar design approaches.

Forward abutment pressure

Forward abutment pressures are characterized by monitoring vertical pressure in the 20th Left longwall panel headgate as shown in Fig. 8A–D. For purposes of discussion, both the BPC pressure readings and pressure changes from equilibrium pressure are presented (Fig. 8 inserts). All pressure cell data are plotted vs. a normalized face distance-to-depth ratio (*Fd/D*).

Onset of the forward abutment is observed when the face approaches within 0.5 to 0.6 of the depth, shows increased rate of vertical pressure rise from 0.1 to 0.2 *Fd/D* and reaches peak vertical pressure when the face is within 0.005 to 0.010 *Fd/D*. Peak vertical pressures ranged from 3.2 to 5.5 times the overburden pressure. The shallower sites, A and B at 1500 ft (450 m), experienced peak pressures of 3.2 and 3.7 times overburden pressure, respectively. The deeper sites, C and D at 2000 ft (600 m), experienced peak pressures of 4.2 and 5.5 times overburden pressure, respectively.

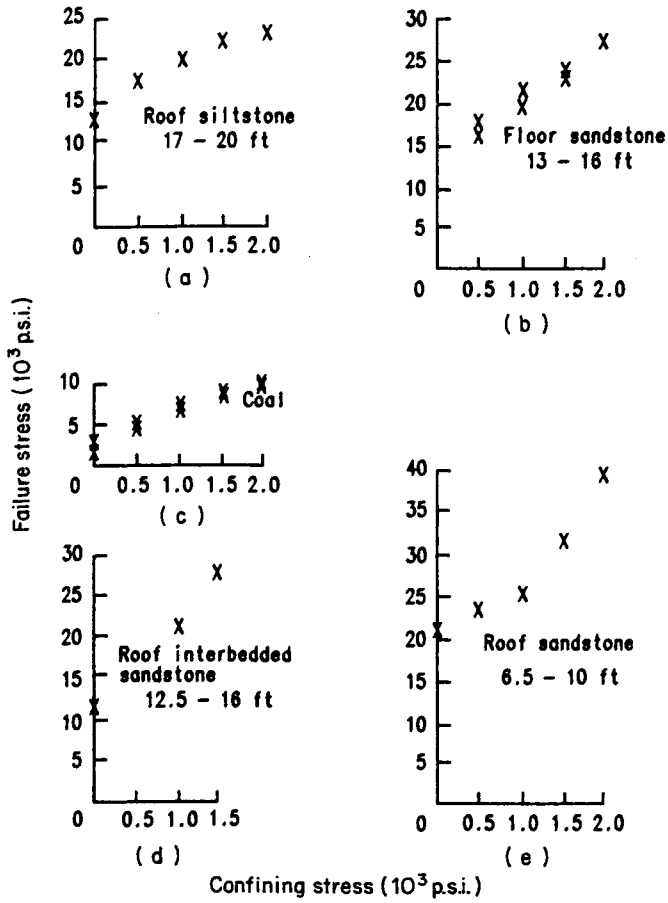

Fig. 7. Triaxial test results from roof, coal, and floor rock (1 ft = 0.3048 m; 1000 p.s.i. = 6.895 MN/m^2). (a) $C_0 = 14\,750$ p.s.i., $K = 4.748$; (b) $C_0 = 13\,900$ p.s.i., $K = 6.608$; (c) $C_0 = 2310$ p.s.i., $K = 4.158$; (d) $C_0 = 9860$ p.s.i., $K = 10.897$; (e) $C_0 = 8600$ p.s.i., $K = 4.158$

Although the above characterizes general behaviour, each site indicated a different response to the approach of mining that may reflect not only overburden depth differences, but also the importance of very localized differences in conditions, e.g. lithology and properties.

Figure 8A, site A, shows an elastic response to forward abutment loading; vertical pressure and vertical pressure change, shown in Fig. 8 were greatest near the rib and decreased with distance into the panel. Site A was the only station that responded elastically to longwall mining; chain pillar and/or panel rib yielding were not observed by the last reading, $Fd/D = 0.04$. Whether a combination of less overburden and locally stronger coal and/or adjacent strata contributed to this anomalous behaviour, or if the pillar eventually yielded at a closer face distance is unknown. Accidental and premature cutting of Site A pressure cell hydraulic lines renders the drawing of firm conclusions impossible

Site B, also at 1500 ft (450 m) depth, does show yielding with approach of the face, Fig. 8B. Unlike site A, the peak stress was measured at 30 ft (9 m) inside the panel rib and occurred

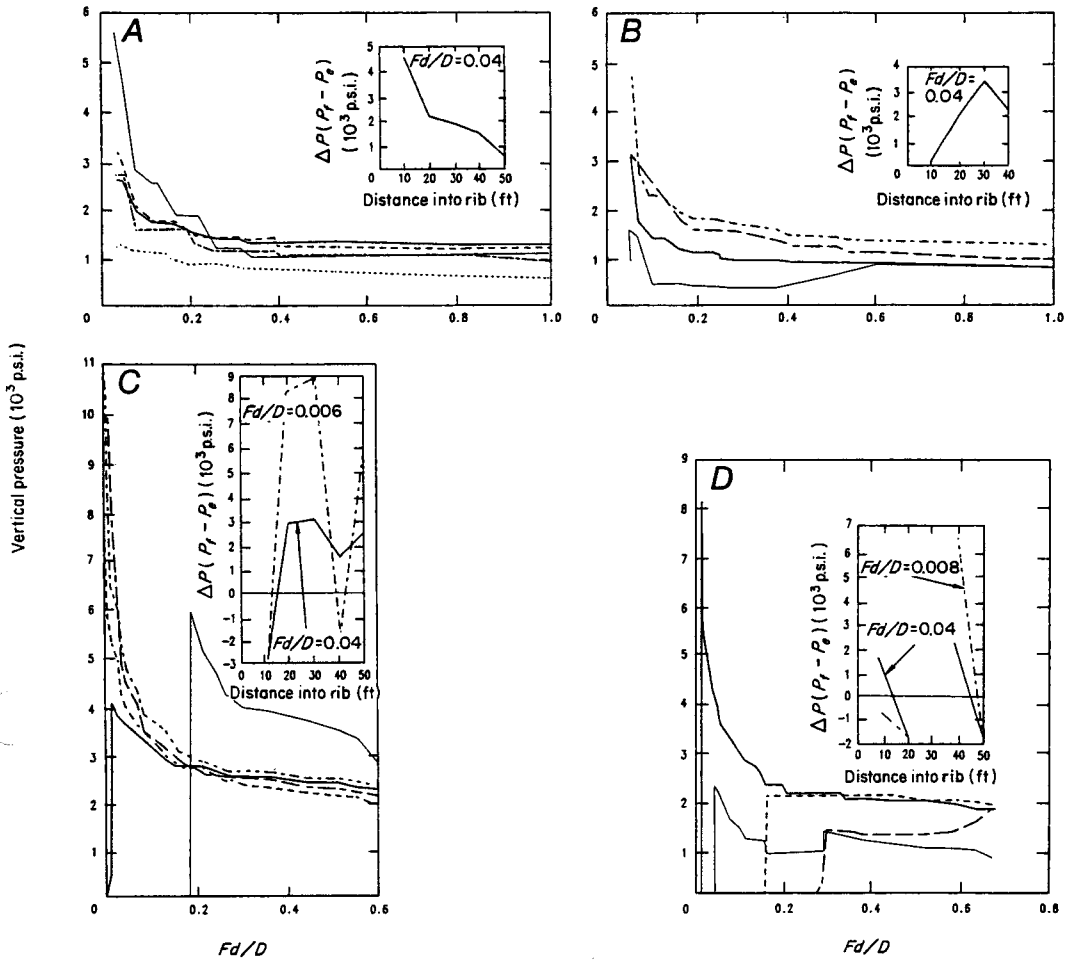

Fig. 8. Headgate mining-induced stress redistribution (1 ft = 0.3048 m; 1000 p.s.i. = 6.895 MN/m²). (-----) 50 ft; (——) 40 ft; (-·——·-) 30 ft; (– – –) 20 ft; (——) 10 ft

only on the shallowest cell. Final readings were recorded when the face was 0.04 *Fd/D* inby, and no conclusions were drawn as to whether additional yielding occurred with approach of the face.

Figures 8C and 8D show not only higher peak vertical pressures at sites C and D, but also deeper yielding into the panel rib than that experienced at the shallower sites A and B. Unlike site A, elastic response, or site B, yielding of panel rib only, sites C and D exhibit a combination of additional yielding to 50 ft (15 m) inside the rib and the existence of highly stressed remnants at shallower depths. Although yielding extended further into the panel rib than was observed at sites A and B, a clearly defined yield zone was not evident; localized high-stress zones still existed when the normalized face distance (*Fd/D*) was 0.006 to 0.008 inby. The pressure change inserts in Figs 8C and 8D show the existence of both locally yielded and locally stressed zones within the headgate rib.

Chain pillar behaviour

Two pillar design concepts are used in mining: (1) the stiff pillar, based on ultimate strength, and sized to fully support the overburden, and (2) the yield pillar, based on progressive failure and sized to transfer load onto stiff, adjacent supports while maintaining stable entries (Tsang *et al.*, 1989).

Longwall mining at Sunnyside No. 1 mine utilizes a two-entry system with a yielding, 32 ft (9.6 m) wide by 100 ft (30 m) long chain pillar. This design, based on experience in bump-prone conditions, has generally been successful in reducing and eliminating the violent failures and roof falls experienced during the early longwall panels. The field study included the installation of BPCs in four chain pillars. The BPC installation was designed to (1) characterize overall pillar response to longwall mining, (2) determine whether the pillars yield, and (3) determine whether yielding occurs, after development or with approach of the longwall face. Field measurements are compared to several yield pillar design concepts to: (1) test predicted vs. *in situ* pillar yielding, and (2) provide a possible explanation for observed differences in behaviour.

Chain pillar vertical pressures are shown in Fig. 9A–9D. Pressure cell readings are plotted vs. the ratio of Fd/D where Fd is the distance from the instrument to the face, and D is the depth at the instrumental site. A broad generalization of observed chain pillar behaviour is difficult; not only are yielding and elastic behaviour observed, but also both development-induced and longwall-induced chain pillar yielding. Pillar A, shown in Fig. 9A, reveals an almost classic elastic stress distribution; high vertical stresses, approximately 6500 p.s.i. (45 MN/m^2) on the panel-side rib, occur at 7 to 8 ft (2.1 to 2.4 m) inside the pillar and surround an elastic core. Unfortunately, the cells were accidentally cut when the face was under 150 ft (45 m) ($Fd/D=0.1$) inby, and no conclusions are shown as to whether this pillar eventually yielded with approach of the 20th Left face.

Pillar B, also under 1500 ft (450 m) of cover and immediately outby pillar A, demonstrates yielding. Pillar ribs yielded before approach of the face, and the pillar core unloaded. The pillar core reloaded with passage of the face and stabilized by the time the face was 300 ft (90 m) ($Fd/D=0.2$) outby.

Pillars C and D, both under 2000 ft (600 m) of cover and located approximately 3000 ft (900 m) outby sites A and B, also demonstrated different behaviour as shown in Figs 9C and 9D. Pillar C indicated pre-longwall yielding of the pillar ribs and load transfer into the pillar core as the face approached. The peak vertical pressure, approximately 3500 p.s.i. (24 MN/m^2), was measured at the centre of the pillar; peak pressure occurred when the face was 400 ft (120 m) inby ($Fd/D=0.2$) and remained essentially constant as the face retreated outby. Pillar D, however, revealed a somewhat elastic response. Peak stresses occurred on the ribs, especially on the rib adjacent to the active longwalls, and an elastic core was revealed. As the face approached within 400 ft (120 m) ($Fd/D=0.2$), the pillar yielded, and the vertical pressures across the pillar decreased to less than 300 p.s.i. (2 MN/m^2).

Observed chain pillar behaviour could be characterized as variable. While three out of four pillars yielded, one pillar behaved elastically. Although readings were terminated prematurely, yielding apparently occurred from both developmental and longwall-induced mining. As various pillar responses were observed, several chain (yield) pillar designs were investigated to determine what, if any, site-specific conditions may have contributed to *in situ* behaviour. Babcock (1985) and Peng and Hsuing (1985) have utilized laboratory studies and numerical modelling allied with field studies, respectively, to investigate the effects of

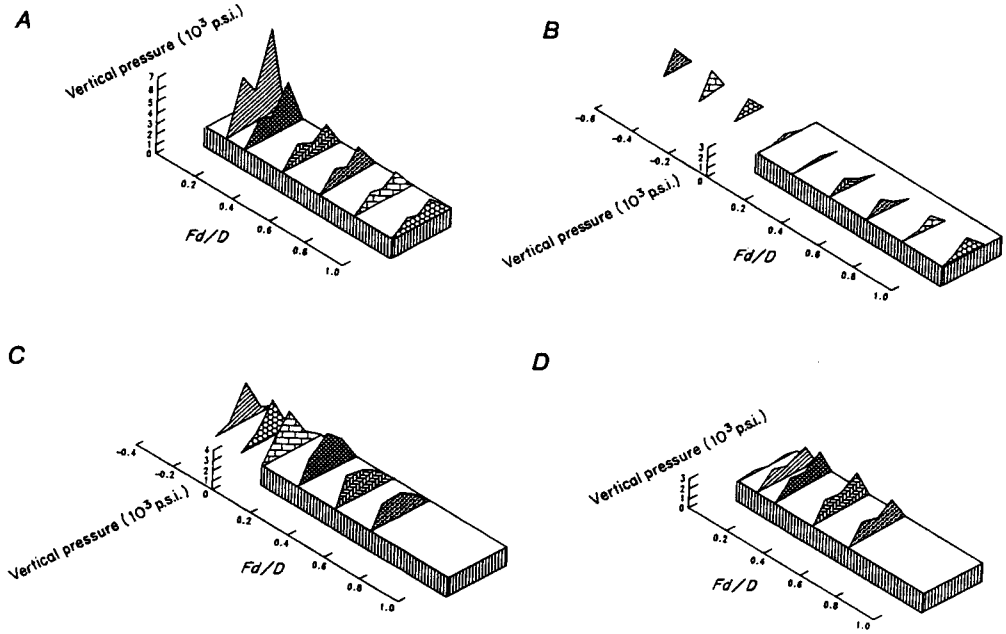

Fig. 9. Chain pillar vertical pressures vs. face distance-to-depth ratio (1000 p.s.i. = 6.895 MN/m^2)

rent roof and floor materials on pillar strength. These studies indicate that relative roof-to-coal and floor-to-coal properties influence not only pillar stability but also failure mode. As variable near-seam lithology, properties, seam thickness, and overburden depths are more often the rule rather than the exception, several yield pillar design concepts that incorporate some of these factors were investigated. Techniques investigated include Wilson's (1972, 1977, 1981) confined core approach and elastic-plastic approach recently proposed by Chen and Karmis (1988, 1989).

Wilson's confined core approach was used to determine whether the chain pillars at the Sunnyside No. 1 mine should yield. Figures 10A–10C show calculated yield zone widths for rigid and yielding roof and floor conditions vs. a range of overburden depths. Yield zone widths for the instrument site depths vs. extraction height variation are also shown. Wilson's equations used are:

$$W = 2X_b = \frac{m}{F} \ln \left(\frac{q}{p + p'} \right)_{\text{(rigid roof-floor)}}$$

$$\text{or} = \frac{m}{2} \left[\left(\frac{q}{p + p'} \right)^{1/K - 1} - 1 \right]_{\text{(yielding roof-floor)}}$$

where X_b = yield zone width, in.
m = seam height, ft
q = overburden load, tsf
p = artificial edge restraint, (0 tsf)

p' = uniaxial strength of fractured coal, 1 tsf

k = triaxial factor $\dfrac{1+\sin\phi}{1-\sin\phi}$

ϕ = angle of internal friction, deg

and $f = f(k) = \left(\dfrac{k-1}{\sqrt{k}}\right) + \left(\dfrac{k-1}{k}\right)^2 \tan^{-1}\sqrt{k}$

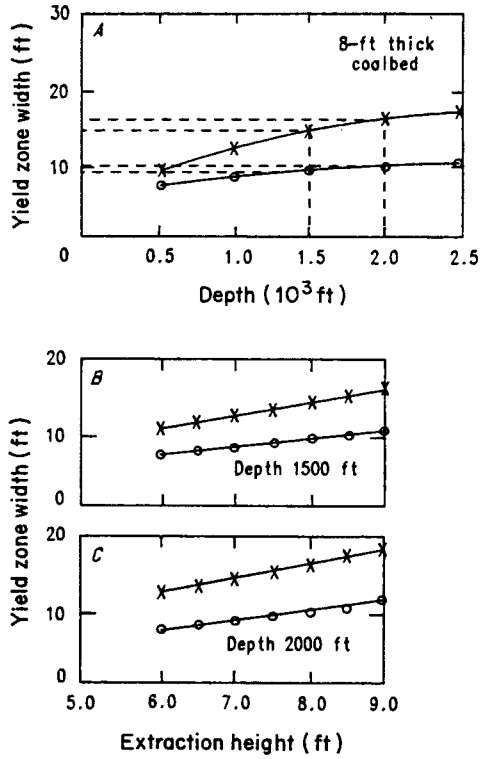

Fig. 10. Calculated yield zones width vs. extraction height using Wilson's equations for an 8 ft thick coal bed (1 ft = 0.3048 m), (○) rigid roof–floor; (×) yielding roof–floor

Figure 10A shows predicted yield zone widths for an 8 ft thick coalbed under a range of overburden depths. As roof rock varied from top coal to sandstone (Fig. 5), yield zone widths were calculated for both rigid roof and floor, and yielding roof and floor configurations. At the test site depths of 1500 ft (450 m) and 2000 ft (600 m), calculated yield zone widths are 9 to 14 ft (3.7 to 4.2 m) and 9.0 to 9.5 ft (2.7 to 2.85 m), respectively. As a yield pillar should be no greater than twice the yield zone width, maximum yield pillar widths should be between 18 to 28 ft (5.4 to 8.4 m), at the 1500 ft (450 m) depth and between 18 to 19 ft (5.4 to 5.7 m) at the 2000 ft (600 m) depth. Figures 10B and 10C illustrate yield zone width dependence upon extraction height variation, a common coal mining condition. At The Sunnyside No. 1 mine, both roof rock and seam height variation could affect chain pillar yielding. Using the rigid roof–floor curves, calculated maximum chain pillar widths are 20 ft and 24 ft (6 and 7.2 m) at

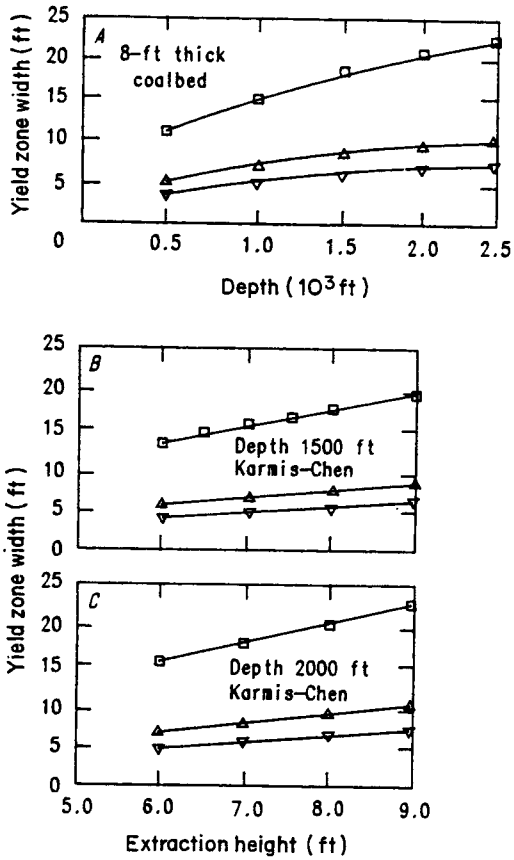

Fig. 11. Calculated yield zone width vs. extraction height using Chen–Karmis equations for an 8 ft thick coal bed (1 ft = 0.3048 m), (□) $\mu = 0.3$; (△) $\mu = 0.4$; (▽) $\mu = 0.5$

1500 ft and 2000 ft (450 m and 600 m) depths, respectively, and the 32 ft (9.6 m) wide design appears oversized. Using the yielding roof–floor curves, and depending upon site-specific seam height, required chain pillar widths varying from 21 to 32 ft (6.3 to 9.6 m) at the 1500 ft (450 m) depths and from 24 to 36 ft (7.2 to 10.8 m) for the 2000 ft (600 m) depths. This curve indicates that with the yielding roof–floor condition, the Sunnyside chain pillars could yield, depending upon the site-specific seam height.

Chen and Karmis (1988, 1989) have recently proposed a progressive failure hypothesis based on elastic-plastic finite-element modelling. Based on a series of computer simulations and subsequent statistical analyses, equations shown below were formulated to calculate pillar stresses and yield zone depths. These equations were developed using the static analysis results with Poisson's ratio range of 0.3 to 0.4.

Chen–Karmis:

$$W = 2X_b = 2H\left\{9.61 \times \cos\left[\frac{1}{3}\cos^{-1}\left(\frac{\gamma h \times 10^{-5}}{f(q)f(\mu)} - 1\right)\right] - 4.8\right\},$$

where X_b = yield zone width, in.

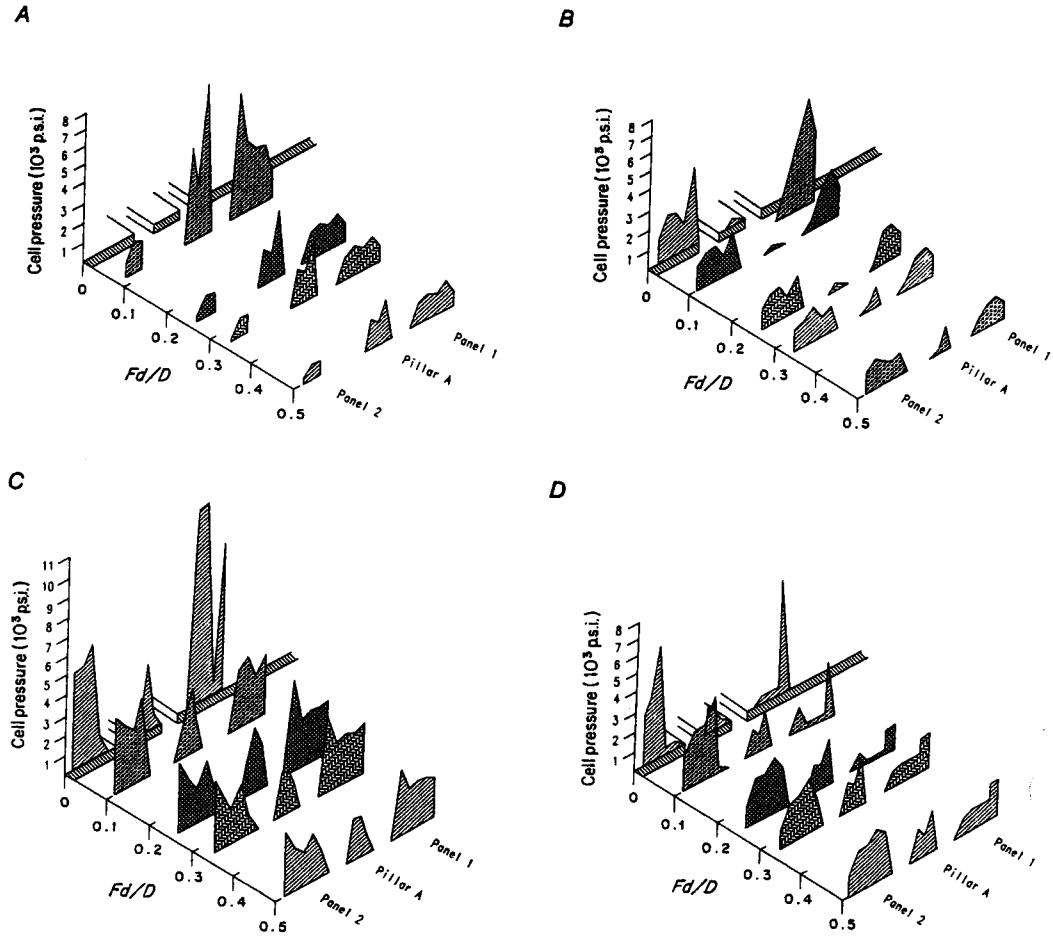

Fig. 12. Vertical cell pressure data for all sites vs. face distance to depth ratio (1000 p.s.i. = 6.895 MN/m²)

γ = average overburden density, p.s.i.
h = depth, in.
H = pillar height, in.
$f(q) = q^{1.7}$

$$q = \text{triaxial factor} = \frac{1+\sin\phi}{1-\sin\phi}$$

ϕ = angle of internal friction, deg
$f(\mu) = -0.28 + 0.057\,\mu + \mu 0.17\,\mu^2$
μ = Poisson's ratio

Yield zone and pillar stress calculations utilize the triaxial factor and Poisson's ratio. Included in this approach is a rationale for sizing yielding pillars: (1) a maximum width based on yield zone extent, (2) a suggested yield width which 'forces' the peak stress to equal

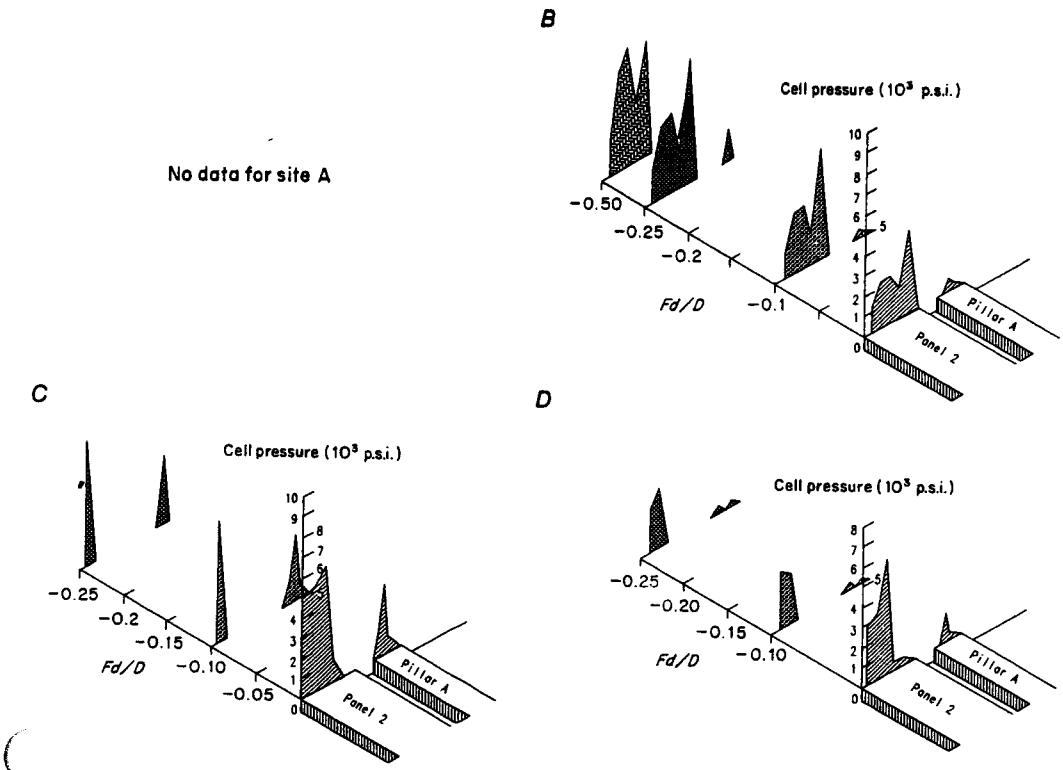

Fig. 13. Headgate stress redistribution following passage of the face (1 p.s.i. = 6.895 MN/m²)

overburden pressure, and (3) a minimum pillar width based on support of the roof under a pressure arch.

In this paper, only maximum yield pillar widths are calculated. The maximum pillar widths are considered critical values; although there is no elastic core, the centre of this pillar will experience high stresses, up to five to six times overburden pressure (Chen and Kamis, 1989). Using laboratory physical property values and relevant mine geometries, calculated yield zone widths using this technique are shown in Fig. 11A–11C.

Figure 11A shows yield zone widths vs. overburden depth. As indicated, Poisson's effect variation can significantly alter estimated yield zone width. Using the site depths and a Poisson's ratio range of 0.3 to 0.5, within the range of laboratory test values, maximum yield pillars widths range from 12 to 35 ft (3.6 to 10.5 m) and from 13 to 40 ft (3.9 to 12 m), at the 1500 ft (450 m) and the 2000 ft (600 m) depths, respectively. As with the Wilson technique, seam height variations also affect yield zone width. With increased height, the required yield pillar width increases for a given Poisson's ratio. With decreased Poisson's ratio, a large yield pillar is required for a given extraction height. The range in extraction heights and Poisson's ratio reflect conditions and properties measured from the Sunnyside No. 1 mine; any one or combination of these could explain the differences in *in situ* behaviour observed in these four instrumented chain pillars.

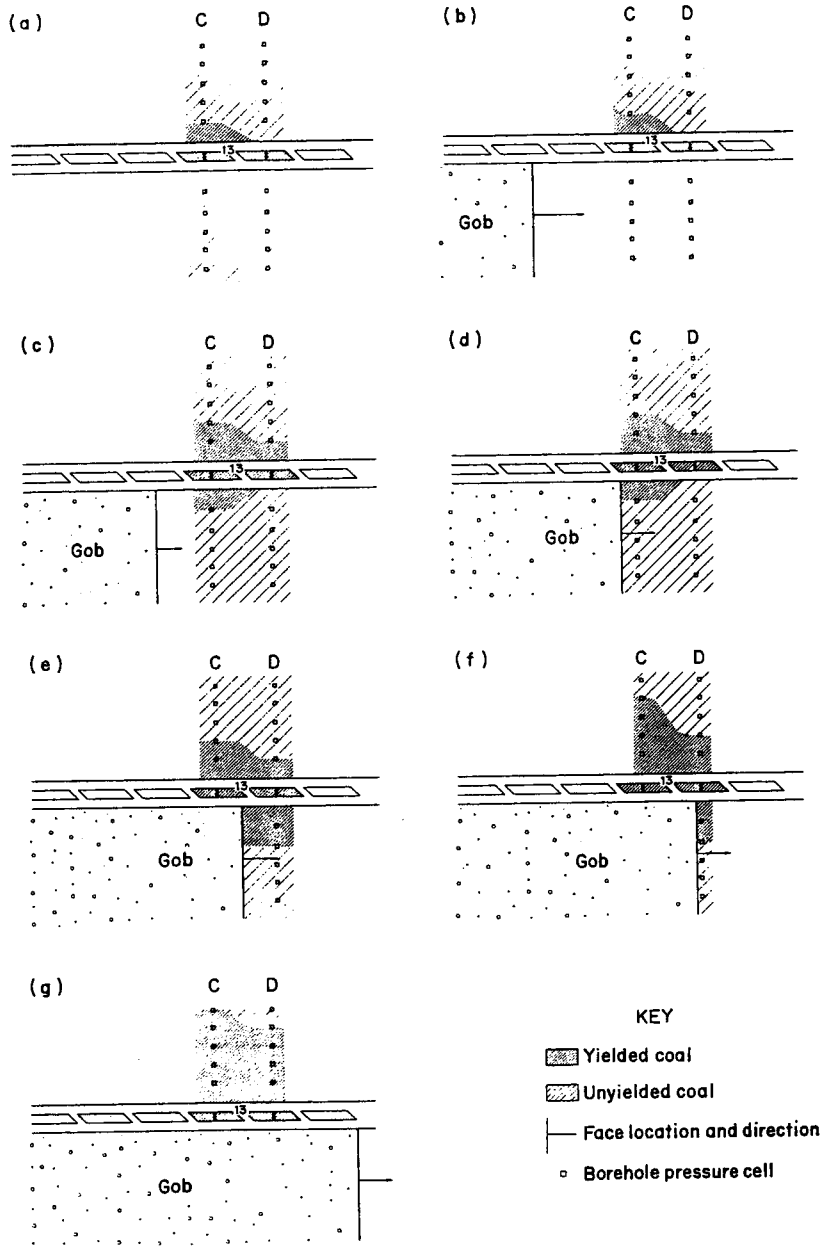

Fig. 14. Mine progression yield sequence obtained from field data (1 p.s.i. = 6.895 MN/m^2)

Stress redistribution over the entries

Structural stability in underground coal mines is highly dependent upon understanding mining-induced stress redistribution. The stress redistribution over the headgate entry pillars and panel for the four sites were plotted vs. the ratio of face distance to depth, Fd/D. The

cal cell pressure data for sites A, B, C, and D are shown in Fig. 12A–D. Figures 13A–D also show the stress redistribution in the longwall entries after passage of the face. No data were available after the face passed site A.

Data analysis indicated that as the face approached the cell locations, pressure in both longwall panels of all stations increased. The cell pressure in the yielding chain pillar, however, did not show any significant increase caused by mining with the exception of site A. No ground control problems were associated with the pressure increase located at the pillar rib in site A. This is an indiction that a pressure arch has developed over the entries which expanded deeper into the panel ribs as the face approached the cells. The entries therefore, were protected from mining-induced stresses and remained stable.

After the longwall passed the instrumented sites, the chain pillars continued to show no increase in load. Stress over the adjacent panel continued to increase although the face was a considerable distance away from the sites. The pressure arch progressed deeper into the rib of the adjacent panel immediately after the longwall passed, and stabilized after the face advanced.

Figure 14 illustrates the progression yielding sequence obtained from pressure cells around stations C and D as mining advanced and passed the instruments. The data illustrate that the headgate end of the mined panel did not yield even when the longwall face was 10 ft inby. This observation was confirmed in the mine where the face remained fairly intact, and coal was dynamically thrown off the face.

Conclusions

Results of this study indicate that the chain pillars at the Sunnyside No. 1 mine generally l as designed, although yielding may not always occur during development. One pillar showed an elastic behaviour when the face was less than 0.1 times the depth inby; whether this pillar subsequently yielded is unknown. Comparison of *in situ* behaviour with some presently available yield pillar design approaches indicates that pillar yielding could occur, but that localized conditions, such as coal and surrounding strata properties, extraction height variations, and changing overburden depths, may significantly influence the behaviour of any one pillar.

Yield pillar designs are shown to have an advantageous stress transfer effect on reducing pressure-related problems in the panel entries. High stresses are eliminated from the chain pillar and panel peripheries; the entries are essentially destressed. With incresed depth, the pressures are shifted further into the panels and the bump potential is reduced.

Although the pillar design methods used do not appear to be completely accurate, they do represent a major step forward and provide a good first estimate for sizing yield pillars. The techniques include physical properties and pillar geometry, this reflects *in situ* conditions and provides a rationale for sizing yield pillars. As yield pillars may become a common feature in future longwalls, goals from a stress control and resource conservation standpoint will include improved understanidng of their behaviour.

References

Babcock, C.O. (1985) Constraint is the prime variable in pillar strength, *Proceedings of the 4th Conference on Ground Control in Mining*, WV Univ., Morgantown, pp. 105–16.

Chen, G. and Karmis, M. (1988) Computer modeling of yield pillar behavior using post-failure criteria, *Proceedings of 7th International Conference on Ground Control in Mining*, West Virginia Univ., Morgantown, pp. 116–25.

Chen, G. and Karmis, M. (1989) An investigation into yield pillar behavior and design consideration, *Proceedings of the Multi-National Conference on Mine Planning and Design*, Kentucky Univ., Lexington, pp. 13–20.

Haramy, K.Y. and McDonnell, J.P. (1988) Causes and Control of Coal Mine Bumps, *BuMines Report of Investigation*, **9225**.

Jackson, Jr., D. (1971) Longwall mining: western style, *Coal Age*, **76**, 72–80.

Lindsay, L.T. (1963) Longwall progress–Sunnyside mines, *Steel and Coal*, **187**, 261–62.

Osterwald, F.W. (1962) U.S.G.S. relates geologic structures to bumps and deformation in coal mine workings at Sunnyside no. 1 mine (Utah), *Mining Engineering*, **14**, 63–8.

Peng, S.S. and Hsiung, S.M. (1985) Chain pillar design for U.S. longwalls, *Mining Science and Technology*, **2**, 279–305.

Peperakis, J. (1968) Multiple seam mining with longwall, *Mining Congress Journal*, **59**, 27–9.

Ross, M.D. (1974) Longwall mining using the single-entry system and advancing tailgate, *Mining Congress Journal*, **60**, 38–41.

Scheibner, B.J. (1979) Geology of the single-entry project at Sunnyside coal mines 1 and 2, Sunnyside, Utah, *BuMines Report of Investigation*, **8402**.

Sunnyside (1962) Sunnyside longwall, *Coal Age*, **65**, 70–4.

Tsang, P., Peng, S.S. and Hsiung, S.M. (1989) Yield pillar application under strong roof and strong floor conditions – a case study, *Proceedings of 30th U.S. Rock Mechanics Symposium*, West Virginia Univ., Morgantown, pp. 411–18.

Wilson, A.H. (1972) A hypothesis concerning pillar stability, *Mining Engineering*, **131**, 409–17.

Wilson, A.H. (1977) The effect of yield zones on the control of ground, *Proceedings of the Sixth International Strata Control Conference, Banff, Alberta*, Energy, Mines and Resources, Canada, Ottawa.

Wilson, A.H. (1981) Stress and stability is coal ribsides and pillars, *Proceedings of First Conference on Ground Control in Mining*, West Virginia Univ., Morgantown, pp. 1–12.

Wong, I.G. (1985) Mining-induced earthquakes in the Book Cliffs and Eastern Wasatch Plateau, Utah, U.S.A., *International Journal of Rock Mechanics, Mining Science, and Geomechanic Abstracts*, **22**, 263–70.